Boosting the host immune system to fight tuberculosis

Boland, R.

3

Identifying host-directed therapeutics against tuberculosis in the zebrafish model

Ralf Boland[1], Michiel van der Vaart[1], Matthias Heemskerk[2], Tom Ottenhoff[2], Herman P. Spaink[1], Annemarie H. Meijer[1]

1. Institute of Biology Leiden, Leiden University, Leiden, The Netherlands
2. Department of Infectious Diseases, Leiden University Medical Center, Leiden, The Netherlands

Abstract

Tuberculosis (TB) remains a global health threat to date, in part because of the rise in multi-drug-resistant *Mycobacterium tuberculosis* (*Mtb*) strains. Host-directed therapeutics (HDTs), currently under investigation as adjunctive therapy for TB, aim to increase the ability of the host-immune system to resist the infection. HDTs have the potential to shorten treatment length with conventional antibiotics and combat multi-drug-resistant TB (MDR-TB). While screens for HDTs using cultured cells can be performed at high-throughput level, the rate limiting step is subsequent validation in whole organism models to translate results to clinical applications. The zebrafish model fills the gap between *in vitro* research and mammalian animal models and is therefore a useful intermediate for translational research. In this study we evaluated a preselected set of compounds with demonstrated anti-TB activity in human cells for a host-directed effect against mycobacterial infection using the zebrafish embryo model for TB. In this well-established model, zebrafish embryos are infected with *Mycobacterium marinum* (*Mm*), a close relative of *Mtb* that displays similar pathogenesis in its poikilothermic hosts. We optimized the infection protocol to determine the most suitable screening conditions. Subsequently, we performed a pilot screen of potential anti-TB HDTs and found Trifluoperazine, Amiodarone-HCl and Tamoxifen-citrate to be effective in the zebrafish model for TB, showing that these compounds not only have anti-TB activity in *Mtb*-infected human macrophages but also in a whole organism test system.

Introduction

Ever advancing technological possibilities have greatly facilitated large-scale *in vitro* screens aimed at the identification of new drugs or cellular pathways as therapeutic targets. An increasing number of screens are performed for a wide range of applications, for example the treatment of cancer and infectious diseases, such as tuberculosis (TB)[1–4]. Furthermore, it has become common practice to re-screen available compound libraries, including FDA-approved compounds, in an effort to repurpose compounds used in therapies for different diseases or not having passed phase-II clinical trials for the disease that they were originally intended for[5–8]. However, research using a whole organism model is always needed to validate discoveries from these *in vitro* screens because disease phenotypes generally result from complex interactions between different cell types. In addition, toxic effects and pharmacokinetics are difficult to assess *in vitro*[9,10]. Furthermore, using a whole organism model could lead to discoveries that would be missed using only *in vitro* screening methods, because of the context of cellular cross-talk in tissues or elaborate pathogen-host dynamics not present when only screening in one cell type. While mammalian models are of great importance for translating research results to clinical applications, the zebrafish model is an effective intermediate for translational research, filling the gap between *in vitro* research and mammalian models[11].

The zebrafish has emerged as an alternative whole organism vertebrate model with a wide range of possibilities, especially for intravital imaging, genetics, and drug efficacy screening. Originally the zebrafish was mainly used to study embryonic development, but since the start of this century it has become a widely used model to study mechanisms of disease, genetic disorders and behavior[12]. Furthermore, many countries have accepted zebrafish as an alternative animal model to study toxicity, in an effort to reduce the number of higher vertebrates used for mandatory safety assessments of chemicals (e.g. in the EU: OECD236 2013).

The popularity of the zebrafish model is easily explained. This small sub-tropical fish can be kept in facilities capable of housing many more animals in the same space

as would be required for mammalian models. They reach a sexual reproductive age in 2 to 3 months. Zebrafish pairs can be crossed every week and a single pair can yield hundreds of eggs in one crossing. The external embryonic development makes the zebrafish highly suitable for experimental manipulation[11]. Genetic modification is performed conveniently by injecting DNA constructs or knockdown/knockout reagents into the zebrafish eggs at the one-cell stage. Owing to these advantages, the zebrafish research community has generated a large number of knock-out as well as transgenic reporter lines, and with technologies such as CRISPR-Cas, the possibilities for genetic interventions have greatly improved[11,13]. Furthermore, temporary knock-down can easily be achieved, for example using synthetic morpholino oligomers[14].

The possibilities of the zebrafish model for various applications, including drug screening, are optimal at the embryonic and larval stages. The zebrafish embryo has a functioning innate immune system as early as 1 day post fertilization (dpf), while it takes at least 3 weeks for the adaptive immune system to fully mature[15]. This means that the early life stages that are extensively used for biomedical research are representative for innate immunity only, thus providing an *in vivo* model to study this branch of the immune system in separation from adaptive immunity[16]. This is especially useful for understanding the interactions between pathogens and phagocytes during the early stages of infection. Furthermore, the transparency of the embryos and larvae, especially when combined with cell lineage-specific promotors driving fluorescent reporters, make zebrafish ideal for real-time fluorescent microscopy studies into cellular and pathogen-host dynamics *in vivo*[17–20].

The aim of this study was to utilize the zebrafish embryo model to screen for potential new host-directed therapeutics (HDTs) for infectious diseases caused by intracellular pathogens. HDTs are drugs that increase the ability of the host's immune system to combat (intracellular) pathogens[21,22]. As such, HDTs could provide an alternative for treatment of antibiotic-resistant infections or be used as adjunctive therapy to enhance the efficacy of antibiotic treatment[23,24]. In our study we infected zebrafish embryos with the intracellular pathogen *Mycobacterium marinum*, which is widely used as a model for TB, caused by its close relative *Mycobacterium tuberculosis* (*Mtb*)[25–27]. TB is a global health threat and the most common cause of death from a single infectious agent, with 1.6 million deaths in 2017 (WHO global report 2018). HDT approaches have attracted much interest in the TB field due to the worrying rise of multiple drug resistant (MDR) strains of *Mtb*, which are unresponsive to several first- and second-line antibiotics. Because of the complex host-pathogen interplay during mycobacterial infection[28–31], the context of a whole organism will be a substantial factor in the translation from *in vitro* HDT screens to clinically relevant drugs. Here, we describe the development of several approaches, as well as identifying potential pitfalls, to screen for anti-TB HDTs using the zebrafish model. Furthermore, we report on results of a pilot screen where we test potential HDTs identified in *Mtb*-infected human macrophages and identify three HDTs effective in the zebrafish model for TB.

Results

Toxicity evaluation of potential anti-TB HDTs

In this study we evaluated the suitability of several *Mycobacterium marinum* (*Mm*) infection protocols for anti-TB drug screening. The list of compounds tested during the course of this study is shown in table 1. These compounds were selected based on previously demonstrated activity against *Mtb* in human MelJuSo cells and primary macrophages (Heemskerk *et al* – in preparation). Before testing compounds under infected conditions in zebrafish, we performed dose range studies to determine the maximum dose tolerated by embryos without induction of overt developmental aberrations. Several compounds induced developmental toxicity, such as oedema

and mortality (Table 1). This precluded us from testing approximately one third of the selected compounds. When subsequently applying non-toxic doses under infected conditions, we generally observed an increase of developmental toxicity. For example, the anti-psychotic drug haloperidol, which does not induce developmental toxicity in absence of infection at doses up to 30 µM, does induce developmental toxicity at this dose when combined with *Mm* infection (Figure 1A), indicating an additive effect of cellular stress caused by drug treatment and infection. It is not surprising that certain HDTs caused toxicity in the zebrafish embryo model for TB as the putative targets of these compounds could be involved in developmental pathways.

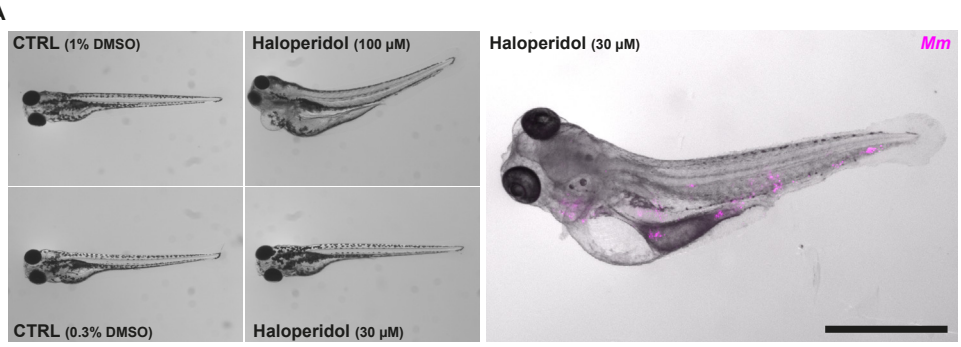

Figure 1. Toxic effects of HDTs are exacerbated by *Mm* infection.

A. Toxicity assay of uninfected and mCherry-expressing *Mm*-infected zebrafish larvae. Zebrafish larvae treated with Haloperidol at mid (30 µM) and high (100 µM) dose or control (DMSO at equal v/v). Treatment was started at 1 hpi and larvae were anesthetized at 4 dpi for imaging. Representative stereo fluorescent images of whole larvae. Right panel shows a larva infected with mCherry-expressing *Mm*. Magenta shows *Mm*. Scale bar annotates 2 mm.

Evaluation of yolk infection and the COPAS system for HDT screens

We wanted to maximize the number of HDT compounds we could screen in a short period of time. For this purpose, we evaluated the Complex Object Parametric Analyser and Sorter (COPAS) system. This system can achieve mid- to high-throughput level in zebrafish embryo screens using fluorescent readouts[32]. Fertilized eggs were infected with *Mm* containing a fluorescent reporter construct at the 8 to 128 cell stage, using a previously described yolk injection route[33]. At 3 dpf, larvae were sorted using the COPAS system and any larvae with infection levels outside the predetermined range as measured by fluorescent readout were discarded. The range of infection level was determined based on a signal higher then background fluorescence of zebrafish larvae, while excluding larvae with a bacterial fluorescent signal above the COPAS detection limit. The remaining larvae were subsequently treated with compounds or vehicle control (DMSO solvent corresponding to the mass percent of the solvent in the final compound concentration) dissolved in the embryo medium (Instant Ocean Sea Salts in demi water). At 2 days post treatment (age 5 dpf), the larvae were again analysed with the COPAS system to quantify the fluorescent signal of *Mm*. By comparing fluorescent signal of the control treatment group to compound treated groups, we obtained a relative measure of bacterial burden and could determine effectiveness of the compound in reducing bacterial burden (Figure 2A). Using this method, we tested several compounds that were found effective in an *in vitro* screen performed on MelJuSo cells infected with *Mtb*, using the antibiotic rifampicin (200 µM) as a positive control for reduction of bacterial burden. We did not identify any compound that effectively reduced bacterial burden, while rifampicin was able to almost clear the infection (Figure 2B). This initial screen included 97i (Table 1), which *in vitro* is a more potent derivative of the kinase inhibitor H89, that has been reported as a potential HDT against *Mtb*[34].

Compound	Toxicity *in vivo* at 10µM dose	*in vivo Mm* screen
Kinase inhibitors		
H89		DoC, BI
97i		COPAS, DoC, BI
98t		
97q		
SB 216763		COPAS
CHIR-99021		COPAS
Imatinib		DoC
ENMD-2076	Oedema	DoC
Dovitinib	Slight oedema	DoC, BI
AT9283		DoC
Quizartinib	Slight oedema	DoC
PDGFR TKI III	Mortality	
GW 5074	Oedema, mortality	
Autophagy modulation		
Spautin-1	Mortality	
Carbamazepine		DoC
Tamoxifen citrate		BI
Amiodarone hydrochloride		BI
Pimozide		BI
Fluspirilene	Slight oedema	COPAS, DoC, BI
Deubiquitinase inhibitors		
M12 (quinazoline)		DoC, BI
C13		
E8		
Trifluoperazine (7994228)		DoC, BI
Chlorprothixene		
Dopamine receptor antagonist		
Haloperidol	Oedema (100n µM dose, excasterbated by *Mm*)	COPAS
Fluphenazine dihydrochloride		BI
cis-(Z)-Flupenthixol dihydrochloride	Mortality	
Golgi apparatus		
Golgicide A	Mortality	COPAS
Exo 1		COPAS
Other		
NBI-74330		DoC

Table 1. Overview of compounds tested
Abbreviations: DoC = Duct of Cuvier and BI = blood island

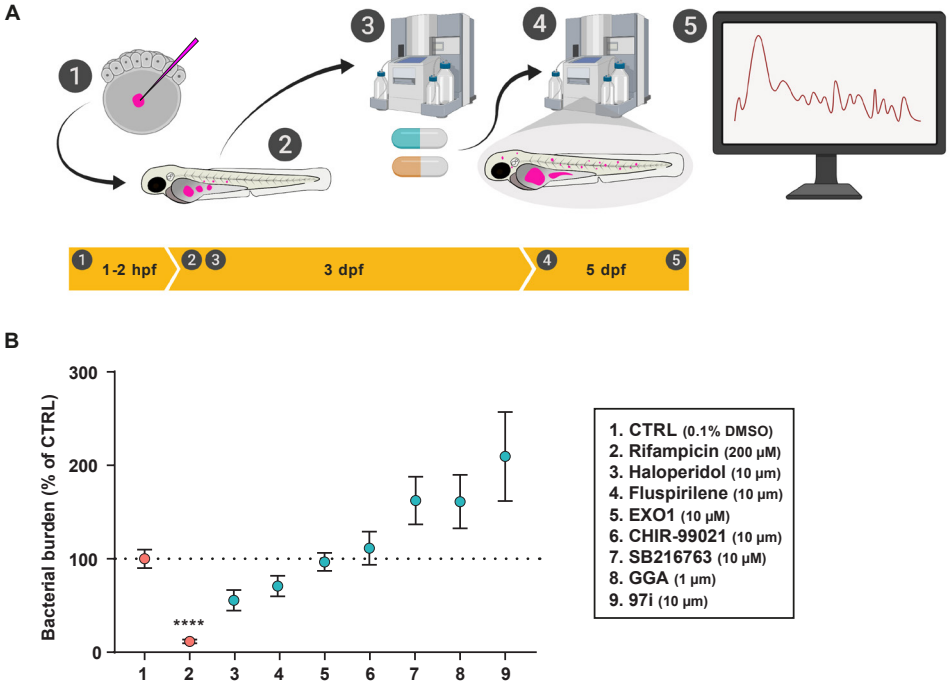

Figure 2. HDT screen using yolk infection and the COPAS system

A. Schematic overview of the experimental procedure of the HDT screen using the COPAS system. Injection of mCherry-expressing *Mm* in the yolk is performed at 8 to 128 cell stage (1). At 3 dpf bacterial burden of larvae are determined by fluorescent readout using the COPAS system (2). Subsequently, larvae are divided in groups and treated with compounds of interest or the control treatment (3). At 5 dpf the COPAS system is again used to determine bacterial burden based by fluorescent readout using the COPAS system (4). Fluorescent signal is obtained per larvae and is a measure of bacterial burden (5). Subsequently, the effect of different treatments on bacterial burden can be compared.

B. Bacterial burden assay of mCherry-expressing *Mm*-infected zebrafish larvae treated with compounds of interests, control treatment (DMSO at 0.1% v/v) or Rifampicin (200 µM) as a positive control for reduction of bacterial burden. Assay was performed as described in A. Normalized data of multiple experiments was included (n = 17-43 per group) and 1 representative control treatment (for both DMSO and Rifampicin) is shown. Dots show mean of each group and error bars indicate standard error of the mean. Statistical analysis was performed per experiment using a Kruskal-Wallis with Dunn's multiple comparisons test. (**** = $p<0.0001$).

Establishment of Duct of Cuvier injection of *Mm* at 2 dpf

While the COPAS system is well suited for fluorescent analysis of zebrafish eggs, embryos and larvae, we did not detect positive effects of any of the HDTs we tested using the yolk infection model. We therefore decided to adopt the more frequently used intravenous infection route for HDT screening using injection into the duct of Cuvier, which leads to rapid phagocytosis of bacteria by macrophages and initiation of TB granuloma formation. Because this procedure is more time consuming than injection into the yolk, quantifying infection using stereo fluorescent microscopy was no longer the bottleneck of the experiment. We therefore replaced the COPAS system and reverted to the use of stereo fluorescent microscopy and fluorescent pixel-count analysis, which has previously been established as a reliable method to quantify infection burden[35]. In this manner we combined bacterial burden analysis with a visual inspection of the larvae for developmental toxicity. To minimize potential developmental toxicity, we decided on an infection timepoint at 2 dpf as opposed to the blood island infection method at 1 dpf used customly in the zebrafish embryo model for TB[36]. We infected 2 dpf embryos in the duct of Cuvier with *Mm*, divided them randomly over treatment groups and treated

with control or compound 1 hour post infection (hpi). At 3 dpi (5 dpf) we imaged the larvae and quantified fluorescent signal using pixel-count analysis (Figure 3A). The experimental end point was set at 5 dpf because of animal experimentation regulation. In light of the relatively short time frame available to assess the effect of a drug on the infection burden, we first assessed *Mm* inoculum doses for the 3 day infection period (Figure 3B). We concluded that a high inoculum dose (400 CFU) maximizes bacterial burden and therefore the potential infection reduction window after HDT compound treatment.

A pilot HDT screen using duct of Cuvier injection did not yield any hits

Having established the screening method by duct of Cuvier injection at 2 dpf, we tested several HDTs that reduced bacterial burden in an *in vitro* screen of MelJuSo cells infected with *Mtb* (Table 1). None of 12 compounds tested reduced bacterial burden in our *in vivo* model, while the antibiotic rifampicin was able to do so (Figure 3C). As H89 and 97i show a synergistic effect with antibiotics *in vitro* (Heemskerk *et al* - in preparation), we hypothesized that these HDTs could potentiate the host in a manner that weakened the bacteria but did not lead to a direct reduction in bacterial burden in our model. We decided to study if a synergistic effect with antibiotics could be achieved using these compounds in our *in vivo* model. Therefore, we treated infected embryos with H89 and 97i alone or in combination with a sub-optimal dose of rifampicin (10-fold lower; 20 µM). We tried a low and high dose of both H89 and 97i. To reduce potential toxic effects of the high doses in combination with Rifampicin, we reduced the treatment window to 2 days and measured bacterial burden at 2 dpi. Both doses of H89 (10 & 50 µM) alone did not reduce bacterial burden compared to control treatment. While a combinatorial treatment of H89 and rifampicin did reduce bacterial burden, the reduction was no greater than treatment with the low-dose rifampicin alone and both treatments did not reduce infection significantly (Figure 3D). Similarly, both doses of 97i (10 & 25 µM) did not reduce bacterial burden significantly, and the reduction in bacterial burden observed in the combinatorial treatment with rifampicin did not exceed treatment with low-dose rifampicin alone (Figure 3D). Although we screened compounds with known *in vitro* HDT potential, we could not confirm the anti-mycobacterial effects of these compounds in our *in vivo* model using the 2 dpf duct of Cuvier infection method.

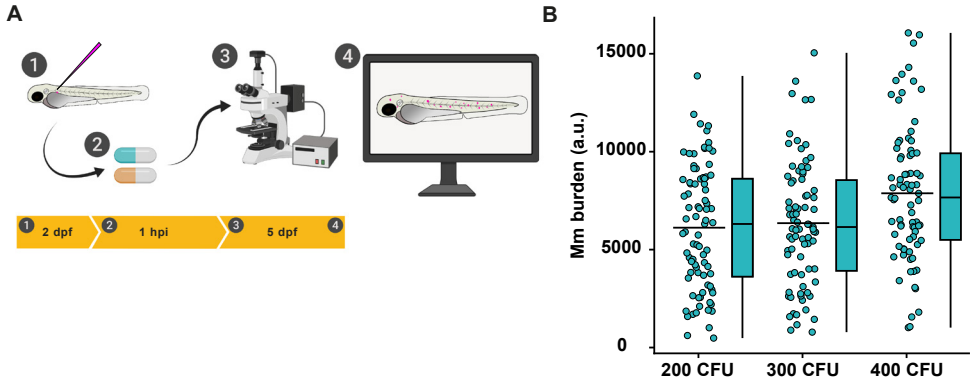

Figure 3. HDT screen using Duct of Cuvier infection

A. Schematic overview of the experimental procedure of the HDT screen using DoC infection. Infection of mCherry-expressing *Mm* in the DoC is performed at 2 dpf (1). Treatment was started at 1 hpi (2) and at 3 dpi larvae were anesthetized and subsequently imaged using a stereo fluorescent microscope (3). Fluorescent signal is obtained per larvae and is a measure of bacterial burden (4). Quantification of fluorescent signal is performed using pixel count analysis.

B. Quantification of bacterial burden as described in A. Infection was performed using an inoculum with increasing CFU. Data of 4 experimental repeats were combined (n = 80-83 per group). Each dot represents a single larva. Boxplots with 95% confidence intervals are shown and the black line in the boxplots and percentage indicates the group median, while the black line in the dot plot indicates the group mean.

Figure and figure legend continued on next page.

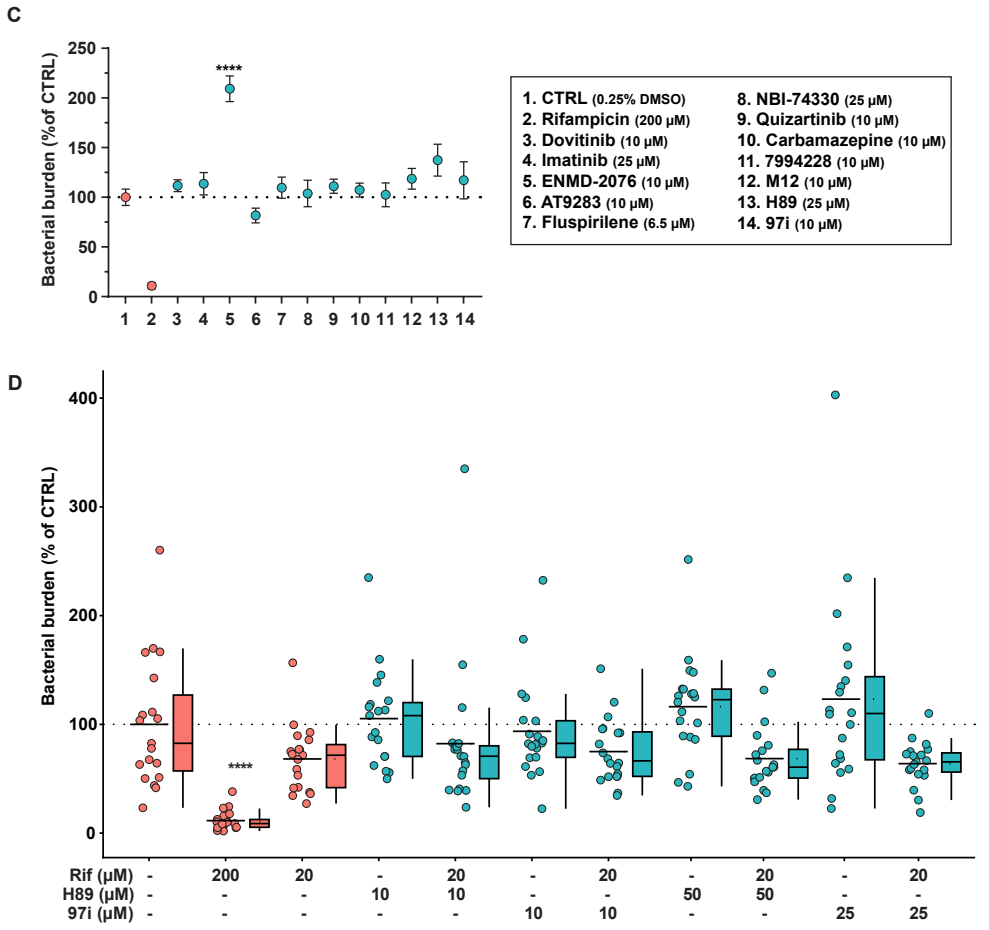

Figure 3. (continued)

C. Bacterial burden assay of mCherry-expressing *Mm*-infected zebrafish larvae treated with compounds of interests, control treatment (DMSO at 0.25% v/v) or Rifampicin (200 µM) as a positive control for reduction of bacterial burden. Assay was performed as described in A. Normalized data of multiple experiments was included (n = 20-31 per group) and 1 representative control treatment (for both DMSO and Rifampicin) is shown. Dots show mean of each group and error bars indicate standard error of the mean. Statistical analysis was performed per experiment using a Kruskal-Wallis with Dunn's multiple comparisons test.

D. Bacterial burden assay of mCherry-expressing *Mm*-infected zebrafish larvae treated with compounds of interests (H89 and 97i) combined with a low dose of Rifampicin (20 µM), control treatment (DMSO at 0.5% v/v) or Rifampicin (200 µM) as a positive control for reduction of bacterial burden. Assay was performed as described in A except the endpoint of the experiment is 2 dpi. Each dot represents a single larva (n = 19-20 per group). Boxplots with 95% confidence intervals are shown and the black line in the boxplots and percentage indicates the group median, while the black line in the dot plot indicates the group mean. Statistical analysis was performed per experiment using a Kruskal-Wallis with Dunn's multiple comparisons test. (**** = p<0.0001).

H89 and 97i do not reduce *Stm* burden in zebrafish

As H89 and 97i did not reduce *Mm* bacterial burden in our zebrafish embryo model for TB, we decided to look at *Salmonella* Typhimurium (*Stm*), another intracellular pathogen causing human disease for which zebrafish embryos and larvae are used as an animal model[37–39]. Previously, H89 and 97i were described to also be effective against *Stm* infection (Heemskerk *et al* – in preparation)[34]. We infected 2 dpf zebrafish embryos with 150 CFU of *Stm*, divided the embryos randomly in treatment groups and treated with control or H89 (25 µM) by adding it to the embryo medium. At 24 and 48 hpi we plated

diluted embryo extractions to get a readout of *Stm* infection burden as measured by colony counting (Figure 4A). We did not find any differences in the number of grown colonies after treatment with H89 at 24 hpi (Figure 4B). Although we did find a significant difference at 48 hpi, at this timepoint most larvae had succumbed to the infection and subsequently died in both the control treated and H89 treated group (Figure 4B). We also injected the compounds directly into the duct of Cuvier to see if this compound delivery method would be more effective than immersion treatment, using a similar approach as described above (Figure 4A). We injected H89 and 97i at high doses (5mM) in the infected zebrafish embryos to get to a tissue concentration around the desired

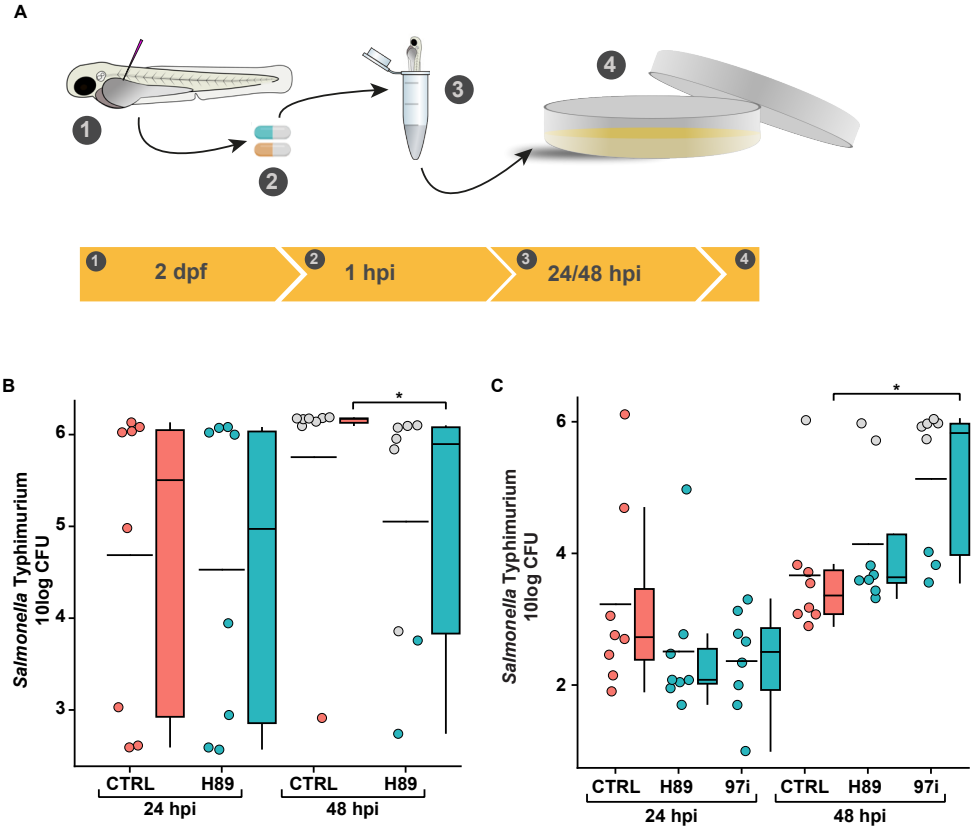

Figure 4. Effect of HDTs on *Stm* burden

A. Schematic overview of the experimental procedure of the HDT screen using *Stm*. Infection of mCherry-expressing *Stm* in the DoC is performed at 2 dpf (1) and treatment was started at 1 hpi (2). At both 24 and 48 hpi larvae (n = 8) were anesthetized and homogenized (3). The resulting homogenates were serial diluted and plated (4). After overnight incubation of the plate, the number of colonies were counted and calculated back to CFU in the original homogenate giving a readout for bacterial burden.

B. CFU assay of mCherry-expressing *Stm*-infected zebrafish larvae treated with H89 (25 μM) or control treatment (DMSO at 0.25% v/v). Assay was performed as described in A. Each dot represents a single larva (n = 8 per group). Boxplots with 95% confidence intervals are shown and the black line in the boxplots and percentage indicates the group median, while the black line in the dot plot indicates the group mean. Grey dots indicate dead larvae. Statistical analysis was performed per experiment using a Mann-Whitney test.

C. CFU assay of mCherry-expressing *Stm*-infected zebrafish larvae treated with H89 or 97i (10 μM) or control treatment (DMSO at 0.1% v/v). Assay was performed as described in A except the treatment was not added to the embryo medium but injected in the DoC. Each dot represents a single larva (n = 8 per group). Boxplots with 95% confidence intervals are shown and the black line in the boxplots and percentage indicates the group median, while the black line in the dot plot indicates the group mean. Grey dots indicate dead larvae. Statistical analysis was performed per experiment using a Kruskal-Wallis with Dunn's multiple comparisons test. (* = $p<0.05$).

treatment dose (10μM). We found similar or higher infection burdens for the H89 and 97i treatment groups compared to the control treatment group at both timepoints and observed high mortality at the 48 hpi timepoint (Figure 4C). We concluded that neither H89 nor 97i are effective in reducing *Stm* burden in our *in vivo* model.

Intracellular infection dynamics

As the HDTs tested in our *in vivo* model were all capable of reducing bacterial load *in vitro* in MelJuSo cells infected with *Mtb*, we analysedintracellular infection dynamics, such as intracellular bacterial load. For this, we utilized the intra-macrophage killing model[40]. Embryos were infected with the less virulent *Mm* ERP mutant strain, and at 24 hpi confocal laser scanning microscopy was used to quantify the number of bacteria

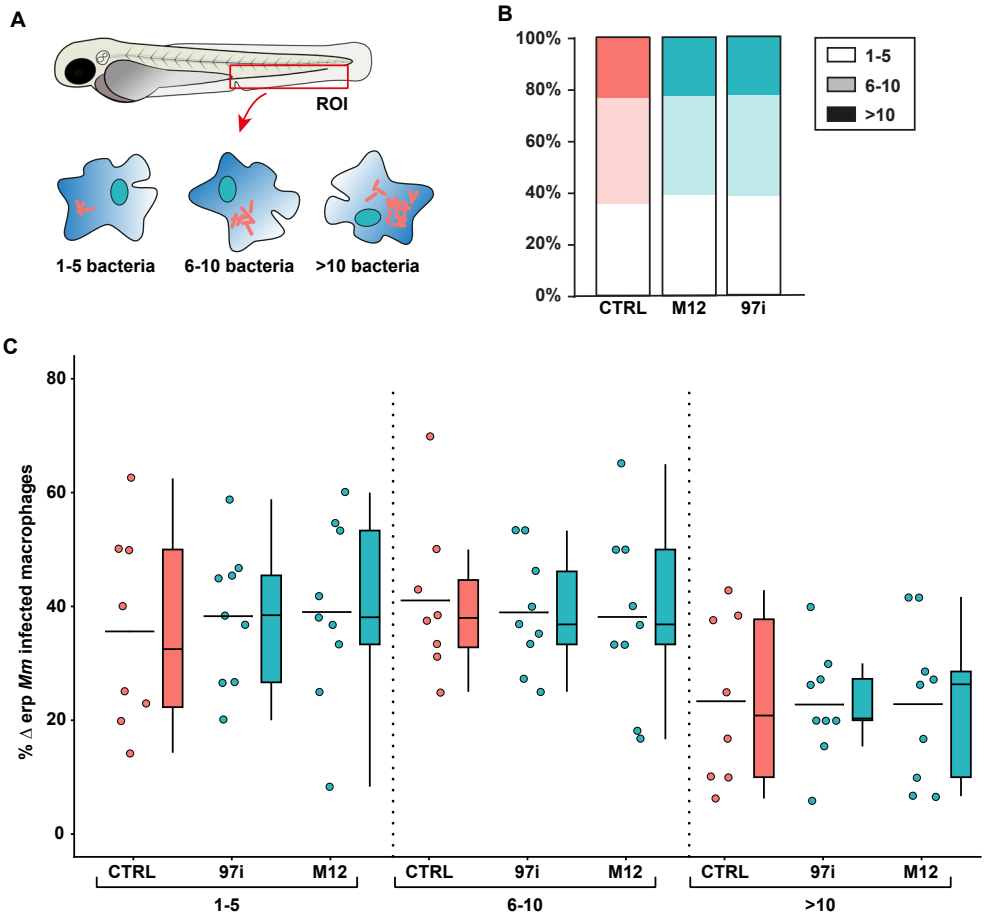

Figure 5. Effect of HDTs on intracellular dynamics of *Mm in vivo* and *in vitro*

A. Schematic overview of the intra-macrophage killing model. A wasabi-expressing *Mm* ERP-mutant-strain was used to infect 30 hpf zebrafish larvae. Treatment was started at 1 hpi and at 2 dpi larvae were fixed using 4% paraformaldehyde and imaged in the CTH region using a confocal microscope. Infected macrophages were classified in low (1-5 bacteria), mid (6-10 bacteria) or high (>10 bacteria) intracellular load.

B. Enumeration of bacteria per macrophage at 2 dpi as described in B comparing larvae treated with M12 (10 μM), 97i (10 μM) or control treatment (DMSO at 0.1% v/v).

C. Quantification of intracellular bacterial load as described in A. Each dot represents a single larva (n = 8-9 per group). Boxplots with 95% confidence intervals are shown and the black line in the boxplots and percentage indicates the group median, while the black line in the dot plot indicates the group mean. Statistical analysis was performed per experiment using a Kruskal-Wallis with Dunn's multiple comparisons test.

Figure and figure legend continued on next page.

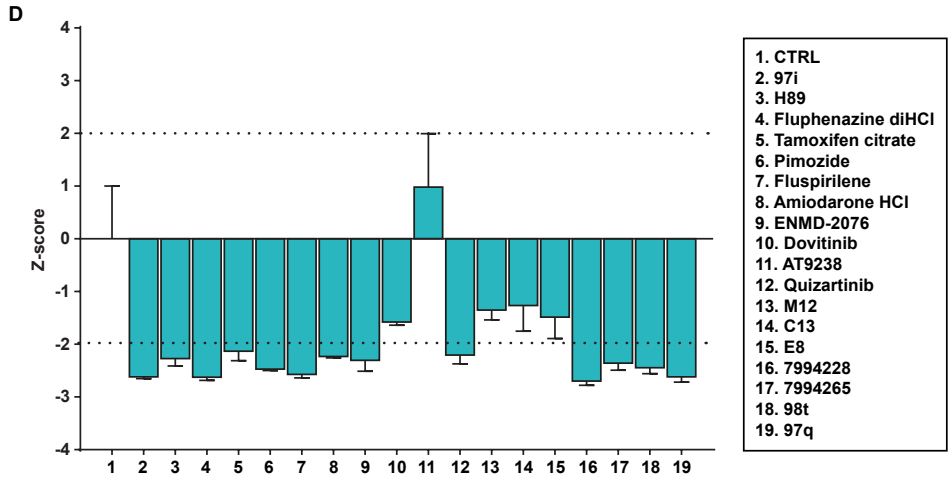

Figure 5. (continued)
D. Bacterial load of mCherry expressing *Mm*-infected MelJuSo cells, expressed as z-scores. Cells were treated with compound of interest (10 µM) or control treatment (DMSO at 0.1% v/v). Bars show average z-score of 3 replicates and error bars indicate standard deviation. The dashed line depicts a cutoff at a z-score of +/−2.

residing in single macrophages in the CHT region of the larvae (Figure 4A). By dividing the intracellular bacterial load of macrophages in three classes of low (1-5 bacteria), mid (6-10 bacteria) or high (>10 bacteria), differences in intracellular survival can be observed. We did not find any effect of 97i or M12 treatment on the number of macrophages distributed over the three classes of bacterial load (Figure 5B-C). We therefore concluded that neither 97i nor M12 increased intracellular killing or inhibited intracellular bacterial growth. We then asked whether differences between *Mm* and *Mtb* pathogenesis and pathogen-host interactions could be the reason why we did not observe reduction of bacterial burden in our *in vivo* model as opposed to the *in vitro* model. Therefore, we infected MelJuSo cells with *Mm* and treated them with a range of compounds known to work in this system with *Mtb* infection. We found almost all compounds to be able to reduce *Mm* bacterial load *in vitro*, including 97i and H89 (Figure 5D). We concluded that differences between the *in vivo* whole organism model and the *in vitro* cell systems were responsible for differences in observed HDT effectiveness, and not differences in the pathogen used.

Back to basics: the blood island infection model yields three hits

As none of the above methods proved effective in screening for HDTs, we decided to return to the blood island infection model commonly used in our laboratory and the zebrafish community[38]. In this model, 30 hpf embryos are infected in the blood island, leading to a systemic infection, similar to that resulting from duct of Cuvier injection. The younger age of the embryos in the blood island method compared to the duct of Cuvier method prohibits testing part of the potential HDT compounds due to developmental toxicity as described earlier (Table 1). However, the younger age at the onset of infection provides a longer time window for evaluation of HDT effects on bacterial burden. After infection via the blood island, embryos were randomly divided in groups. At 1 hpi, treatment was performed by immersion in embryo medium containing the compounds. Stereo fluorescent imaging at 4 dpi and subsequent pixel-count analysis was used to quantify bacterial burden of the different treatment groups (Figure 6A). We decided to test selected compounds from an autophagy modulating library and a deubiquitinase inhibitor library. These compounds were identified as hits *in vitro* in *Mtb*-infected MelJuSo cells as well as in *Mtb*-infected human primary macrophages

(Heemskerk *et al* – in preparation). While neither H89 nor 97i showed marked activity in the blood island infection model, we found 1 compound from the DUB inhibitor library (Trifluoperazine) and 2 compounds from the autophagy modulating library (Amiodarone-HCl and Tamoxifen-citrate) to be effective in initial screens (Figure 6B). Therefore, we conclude that the 1 dpi blood island infection method, which provides a window of 4 days to assess drug efficacy, is a practical procedure for HDT screening, resulting here in the identification of several promising candidates for further research.

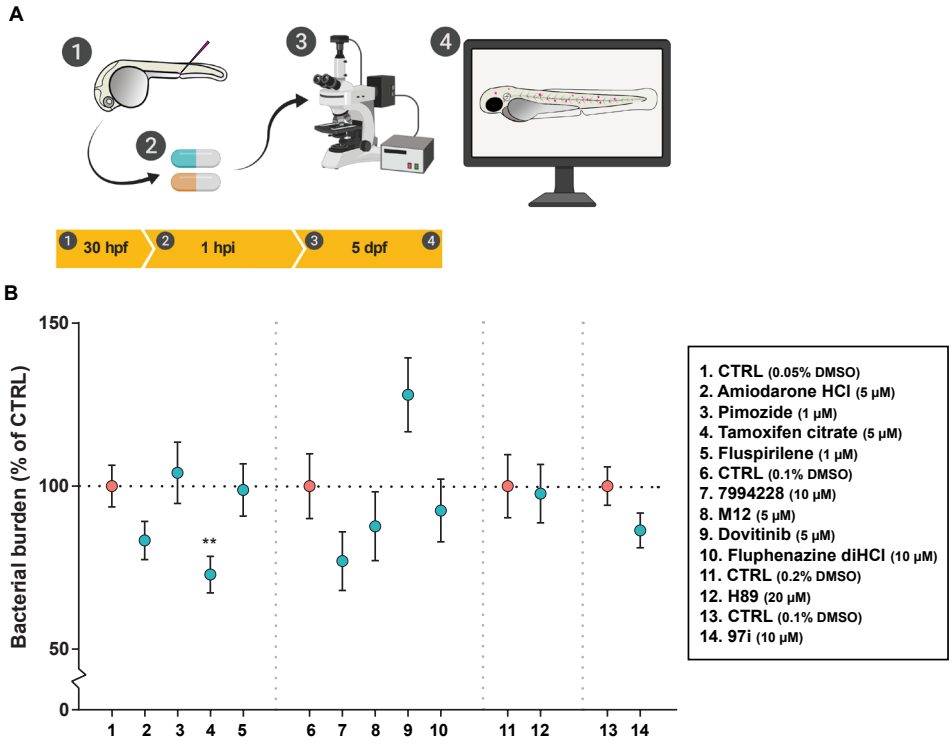

Figure 6. HDT screen using blood island infection model

A. Schematic overview of the experimental procedure of the HDT screen using blood island infection. Injection of mCherry-expressing *Mm* in the blood island is performed at 30 hpf (1). Treatment was started at 1 hpi (2) and at 4 dpi larvae were anesthetized and subsequently imaged using a stereo fluorescent microscope (3). Fluorescent signal is obtained per larvae and is a measure of bacterial burden (4). Quantification of fluorescent signal is performed using pixelcount analysis.

B. Bacterial burden assay of mCherry-expressing *Mm*-infected zebrafish larvae treated with compounds of interests or control treatment (DMSO at equal v/v). Assay was performed as described in A. Normalized data of multiple experiments for each treatment was included (n = 2-4). Dots show mean of each group and error bars indicate standard error of the mean. Black dotted line indicates control mean set at 100%. Grey vertical dotted lines indicate multiple experiments. Statistical analysis was performed per normalized dataset using either a Kruskal-Wallis with Dunn's multiple comparisons test for experiments or a Mann-Whitney test for datasets with more than 2 treatment groups or datasets with 2 treatment groups respectively. (** = $p<0.01$).

Discussion

Large scale screening using cell-based assays is increasingly utilized to identify potential new therapeutic approaches[1]. Many screens aim at repurposing of FDA-approved drugs or compounds that have not passed phase-II clinical trials for their originally intended use[7,8]. However, cell-based assays cannot mimic all aspects of a disease and it is difficult to assess developmental toxicity and tissue-relevant effects using cell cultures. While screens using three-dimensional culture models aim to address these limitations, animal models will remain a vital step towards new therapeutics[10]. The zebrafish has filled the gap between cell-based assays and mammalian models as a medium throughput and cost-effective animal model to identify new therapeutic approaches[41–44]. Our aim was to screen for anti-TB HDTs using the well-established zebrafish embryo model for TB[25–27].

We initially attempted an approach that could potentially be scaled up and partly automated by using robotic injection[32,33]. However, the yolk infection approach did not yield any HDT hits, contrary to the antibiotic rifampicin that was used as a positive control for reduction of bacterial burden. For HDTs to work effectively, the host immune system must interact with the pathogen. This interaction is not needed when testing antibiotics that target bacteria directly regardless of the tissue environment of the infection. In the yolk infection model, interaction between pathogen and the innate immune system only starts at 2 to 3 dpf (2 to 3 dpi) when *Mm* is able to infect tissues in the developing embryo[33]. As a consequence, the yolk remains a safe reservoir for *Mm* throughout the experimental window, as immune cells do not migrate in the yolk and the yolk provides a rich source of nutrients for *Mm*[45]. We therefore abandoned the use of the yolk infection model and turned to intravenous injection routes that are known to result in rapid phagocytosis of *Mm* by macrophages[19,38,46].

We compared two types of intravenous infection, the duct of Cuvier infection route at 2 dpf, and blood island infection route at 1 dpf. By imaging the larvae using stereo fluorescence microscopy, we could assess bacterial burden and potential developmental toxicity at the same time in both methods. This led us to conclude that embryos are more sensitive to developmental toxicity when drugs are applied from 1 dpf compared with 2 dpf. Thus, developmental toxicity can be minimized using the duct of Cuvier method. However, the duct of Cuvier method provides only a 3 day experimental window, while the blood island method allows us to follow the disease progression over 4 days. This is due to the fact that the end point of both methods is set at 5 dpf because of animal experimentation regulation. We used both methods to test kinase inhibitors (H89, 97i), shown to be effective in human cells against not only *Mtb* but also *Mm* and *Stm* (this study)[34]. These drugs could not reduce overall bacterial burden of *Mm*-infected or *Stm*-infected zebrafish. More detailed analysis of intracellular pathogen-host dynamics using a zebrafish *in vivo* intra-macrophage killing model also did not reveal an effect of the kinase inhibitor 97i or the deubiquitinase inhibitor M12. We decided to use the 1 dpf blood island infection model to perform pilot screens of potential HDT candidates with demonstrated effectivity against *Mtb* and *Mm* in human cells. Using this model, we found the HDTs Trifluoperazine, Tamoxifen and Amiodarone to reduce bacterial burden.

Tamoxifen targets the estrogen receptor either as an agonist or as an antagonist, depending on the tissue. It is widely used in the clinic for breast cancer therapy. Furthermore, it has been studied in the context of various infections, such as Cryptococcus, toxoplasma and Leishmania[47–49]. There is also previous evidence for a link with TB, since Tamoxifen was found to have direct anti-mycobacterial activity, also on drug-resistant strains, as well as a synergistic effect with first-line anti-TB drugs[50,51]. The question remains if the effect we observe on mycobacterial burden is host-directed and related to the estrogen receptor, or if different host pathways are modulated for the anti-mycobacterial effect. Tamoxifen was identified by screening an autophagy-modulating compound library and indeed autophagy can be modulated by Tamoxifen treatment[52]. Autophagy is an intracellular degradation pathway vital to maintaining

homeostasis by removing unwanted elements from the cell, such as misfolded protein aggregates and damaged organelles but it has also been shown to be a defense mechanism against microbial invaders[53–55]. Modulation of the autophagy pathway could be the reason for the observed effect of Tamoxifen and this will be investigated in future research (Chapter 4).

Amiodarone is an adrenergic receptor inhibitor and it blocks myocardial calcium, sodium and potassium channels. Furthermore, Amiodarone induces nitric oxide (NO) production, which is known to play a role in combating mycobacterial infection via production of reactive nitrogen species[56–58]. Like Tamoxifen, Amiodarone was identified by screening an autophagy-modulating compound library and has been shown to induce autophagy[59,60]. In contrast to Tamoxifen, Amiodarone has not been previously linked to TB. Amiodarone could work in a similar manner as Tamoxifen by modulating the autophagy pathway or alternative a host directed effect, such as NO production, could be the mechanism behind the anti-mycobacterial effect. Further research efforts will be required to elucidate its mechanism of action (Chapter 5).

Trifluoperazine was identified by screening a library of deubiquitinase inhibitors (Heemskerk *et al* – in preparation). In general, ubiquitin is attached to intracellular cargo such as proteins to mark them for degradation and deubiquitinases facilitate deubiquitination, the removal of this ubiquitin signal[61,62]. During TB pathogenesis, mycobacteria are capable of escaping phagosomes and can subsequently be ubiquitinated and targeted for selective autophagy via ubiquitin receptors[55]. Our lab has recently shown that this mechanism is important for host defence in zebrafish, as mutants in the ubiquitin receptors p62 and optineurin are hypersusceptible to *Mm* infection[63]. As a survival mechanism, intracellular pathogens will benefit from deubiquitination. Indeed, *Stm* has been shown to excretes the deubiquitinase SseL and is thereby able to inhibit selective autophagy[64]. In the case of Trifluoperazine it remains to be investigated which deubiquitinase(s) is (are) inhibited and if these are host or pathogen derived.

We show that the zebrafish model for TB can be used to identify HDTs with anti-mycobacterial effects, however we found that in several cases results obtained by cell-based culture assays did not translate to *in vivo* anti-mycobacterial effects in the zebrafish model. There are several possible explanations for differences between human cell-based and zebrafish *in vivo* screens. Some drugs identified in cell-based screens using *Mtb* might fail to reduce *Mm* burden in zebrafish for example because of differences between the pathogens or lack of conservation of the drug target site. However, a screen in zebrafish could identify drugs that act at later stages of diseases progression, for example acting on targets involved in granuloma development. Such drugs would never be identified in a cell-based screen. Furthermore, it cannot be excluded that many of the hits from cell-based screens are simply not relevant due to the phenotypic changes that mycobacteria undergo during the process of granuloma formation[25,65,66]. Proper evaluation of different screening methods awaits translation of results from cell-based screens to animal models, including the zebrafish and mammalian models.

Developmental toxicity prevented us in several cases from validating HDTs in zebrafish. For example, haloperidol was shown to reduce intracellular *Mtb* survival in human cells[67], while treatment of *Mm*-infected zebrafish embryos led to massive oedema (this study). We were also unable to confirm the antibacterial effects of Imatinib and H89, drugs that target kinases. H89 was shown to work on both *Mtb* and *Stm* in cell-based and mouse models[34], but did not restrict *Mm* or *Stm* infection burden in the zebrafish model. Similarly, imatinib did not show reduction of *Mm* bacterial burden in the zebrafish model, though it was found effective in cell-based and mouse models against *Mm* and *Mtb*[68]. Differences in these results from cell-based and mouse models compared to the zebrafish model might be attributed to side effects due to roles of the target kinases in developmental processes. For instance, Imatinib is thought to target ABL family tyrosine

kinases and these have been shown to have important roles in zebrafish development[69]. In contrast, compounds that putatively target ubiquitination and autophagy processes (Trifluoperazine, Tamoxifen and Amiodarone) worked in cell-based assays against *Mtb* as well as against *Mm* in the zebrafish model, providing *in vivo* validation for these compounds (this study). Another successful example of a screen performed in zebrafish resulted in the identification of HDT Clemastine, which is capable of restricting *Mm* infection *in vivo* in zebrafish larvae and *ex vivo* in zebrafish granuloma explants, possibly by affecting inflammasome signaling[44]. It remains to be established if this drug also works in human cell based or mammalian models and if this drug could go to clinical trials for use in TB patients.

Drug uptake and metabolism is another important aspect to take into consideration. A great advantage of the zebrafish model is the simplicity of treatment by adding drugs to the embryo medium. However, for this to work HDTs need to be water soluble, while metabolites or the HDTs themselves might alter pH of the embryo medium. To prevent this, we replaced normal embryo medium with a buffered embryo medium (1X E2). Characteristics of HDTs, such as size, molecular weight and lipophilicity, will influence the potential uptake of HDTs by the zebrafish embryo[70]. Because the mouth of zebrafish embryos opens around 3 dpf, initial uptake of nutrients, oxygen and subsequently any drug treatment is mediated mostly by diffusion through the skin. It remains unclear how concentrations in the embryo medium relate to *in vivo* concentrations, although it is assumed to reach similar levels. Advances in deducing pharmacokinetics of the zebrafish model will shine more light on this aspect. For instance, it has been shown that uptake and metabolism of paracetamol in the zebrafish model translates well to what is known of human pharmacokinetics of paracetamol[71,72]. Nevertheless, inefficient uptake or inactivation of the drug through metabolism could have been a cause of false negatives in our screen.

The zebrafish model has distinct advantages as an intermediate whole organism screening model between cell-based systems and mammalian models. Although predicted HDT targets or described effects can be indicators of the mechanistic function of an HDT, it remains unclear how the hits obtained in our screen exert their anti-mycobacterial effects and further studies into the mechanism of action are required. The zebrafish model is useful not only for the drug screening process but also for subsequent mechanistic studies, which will benefit from efficient genetic tools and excellent possibilities for intravital imaging of host-pathogen interactions.

Materials & methods

Ethics statement

Zebrafish were maintained and handled in compliance with the local animal welfare regulations as overseen by the Animal Welfare Body of Leiden University (license number: 10612). All practices involving zebrafish were performed in accordance with European laws, guidelines and policies for animal experimentation, housing and care (European Directive 2010/63/EU on the protection of animals used for scientific purposes). The present study did not involve any procedures within the meaning of Article 3 of Directive 2010/63/EU and as such it is not subject to authorization by an ethics committee.

Zebrafish husbandry and handling

Wild type zebrafish (AB/TL) were maintained according to standard protocols (www.zfin.org). Zebrafish eggs were obtained by natural spawning of single crosses to achieve synchronized developmental timing. Eggs from at least 5 couples were combined to achieve heterogeneous groups. Eggs and embryos were kept in egg water (60 µg/ml

sea salt, Sera Marin, Heinsberg, Germany) or E2 buffered embryo medium (composition: 15 mM NaCl, 0.5 mM KCl, 1 mM $MgSO_4$, 150 µM KH_2PO_4, 1 mM $CaCl_2$ & 0.7 mM $NaHCO_3$) at ~28.5 °C for the duration of experiments, with the exception of necessary handling for experimental procedures.

Bacterial strains and inoculum preparation

Mycobacterium marinum (*Mm*) M-strain or ERP-mutant strain containing a construct with a green (Wasabi) or red (mCherry) fluorescent reporter and resistance for selection (hygromycin) was used for infections[40,46]. Fresh inoculum was prepared for every infection experiment as described[38]. Briefly, the inoculum was created from 10 ml of overnight liquid culture (7H9 containing ADC and 50µg/ml hygromycin) grown at ~28.5 °C. Final inoculum was resuspended in 1X PBS containing 2% (w/v) polyvinylpyrrolidone (PVP40). Injection dose in colony forming units (CFU) was determined by optical density measurement (OD_{600} of 1 corresponds to ~100 CFU/nl) of a 1:10 dilution to ensure accurate measurements (OD_{600} < 1). In the case of the ERP-mutant strain, where single-use aliquots containing single cell suspensions were necessary, these were prepared as previously described and kept at -80 °C[40].

Salmonella **Typhimurium** (*Stm*) SL1344-strain containing a construct with a red (mCherry) fluorescent reporter and resistance for selection (streptomycin and kanamycin) was used for infections[73,74]. Fresh inoculum was prepared for every infection experiment as described[39]. Briefly, the inoculum was created from resuspending a colony from an overnight agar plate (LB containing 90µg/ml streptomycin and 50µg/ml kanamycin) in 1X PBS containing 2% PVP40. Injection dose in CFU was determined by optical density measurement (OD_{600} of 0.5 corresponds to ~200 CFU/nl).

Zebrafish embryo infections

Below is a brief description of previously published injection techniques that were used for infection experiments[33,38,40]. All injections were performed using borosilicate glass microcapillary injection needles (Harvard Apparatus, 300038, 1 mm O.D. x 0.78 mm I.D.) prepared using a micropipette puller device (Sutter Instruments Flaming/Brown P-97). Needles were mounted on a micromanipulator (Sutter Instruments MM-33R) connected to a stand (World Precision Instruments M10L) and positioned under a stereo microscope (Leica M50). Prior to injection, embryos were anesthetized using 200 µg/ml buffered 3-aminobenzoid acid (Tricaine, Sigma-Aldrich) in egg water. After infection, embryos were incubated at ~28.5 °C in fresh egg water or E2.

Yolk infection**:** eggs between the 8 and 128 cell stage were positioned on a 1% agarose (in egg water) plate containing slots and injected in the centre of the yolk with an inoculum of 1 nl containing ~30 (CFU). Any damaged eggs were discarded 2 to 6 hours post infection (hpi).

Duct of Cuvier infection**:** 2 days post fertilization (dpf) old embryos were positioned on a 1% agarose (in egg water) plate prior to injection in the duct of Cuvier with an inoculum of 1 nl containing ~200 to ~400 CFU *Mm* or *Stm* (CFU dose is described for each individual experiment).

Blood island infection**:** 30 hours post fertilization (hpf) embryos were positioned on a 1% agarose (in egg water) plate prior to injection in the blood island with an inoculum of 1 nl containing ~200 CFU *Mm*. For the intra-macrophage killing model, blood island injection was performed similarly except the inoculum of single-cell *Mm* ERP-mutant strain was obtained from single-use aliquots kept at -80 °C as described above.

Compound treatment of zebrafish embryos

All compounds were dissolved in 100% DMSO (D8418, Sigma Aldrich) in stock concentrations of 10 mM, aliquoted and kept at -80 °C. Treatment of embryos was performed by immersion with exception of the *Stm* injection experiment (Figure 4C). Stock concentrations were diluted to treatment doses in egg water (Figure 1-4), which was replaced during the course of the study by 1X E2 (Figure 6). As a solvent control treatment, 100% DMSO was diluted to the same concentration of the compound treatment in either egg water or E2. If multiple compound treatment doses were used

in the same experiment, the solvent control concentration corresponding to the highest compound treatment dose was used. Exact doses of compound treatment and solvent control concentration are described for each individual experiment. For the yolk infection experiments, treatment was performed 3 days post infection (dpi) until the endpoint of the experiment at 5 dpi. For the duct of Cuvier *Mm* infection experiments, treatment was performed 1 hour post infection (hpi) until the endpoint of the experiment at 2 or 3 dpi. For the blood island infection experiments, treatment was performed 1 hpi until the endpoint of the experiment at 4 dpi. For toxicity assessment, treatment was performed at 1 hpi or 2 dpf. For the intra-macrophage killing model, treatment was performed at 1 hpi until the endpoint of the experiment at 2 dpi. For *Stm* infection experiments, treatment was performed 1 hpi either by immersion or by injecting PBS diluted stock concentrations 1 hpi in the duct of Cuvier, assuming a 500X dilution in the tissue to achieve the desired treatment dose.

Bacterial burden assessment of infected zebrafish embryos

***Yolk infection*:** larvae were anesthetized using tricaine at 3 dpi and run through the Complex Object Parametric Analyzer and Sorter (COPAS) system to measure bacterial fluorescent signal. Any larvae having too little or too high infection as measured by fluorescent readout were discarded. At 5 dpi treated larvae were anesthetized using tricaine and run through the COPAS system again to measure bacterial fluorescent signal[33].

***Duct of Cuvier and blood island infection*:** larvae were anesthetized using tricaine at 3 dpi (duct of Cuvier) or 4 dpi (blood island), positioned on a 1% agarose (in egg water) plate and imaged using a Leica M205 FA stereo fluorescence microscope equipped with a DFC345 FX monochrome camera. Bacterial burden was assessed using dedicated pixel quantification software[35].

***Intra-macrophage killing*:** larvae were fixed using 4% paraformaldehyde in PBS at 44 hpi and subsequently intra-macrophage mycobacterial sites of growth were counted using a Zeiss Observer 6.5.32 confocal microscope with a C-Apochromat 63x/1.20 W Korr UV-VIR-IR M27 objective.

***CFU counts*:** At each timepoint 8 embryos/larvae were put in individual Eppendorf tubes in 100 µl of 1X PBS with beads (1.0 mm zirconium oxide, Next Advance) and homogenized using a tissue homogenizer (Bullet Blender, Next Advance). Homogenates were serial diluted and 10 µl of each dilution was spotted twice on an agar plate (LB containing 90 µg/ml streptomycin and 50 µg/ml kanamycin) that was incubated at 37 °C overnight. Spots of the dilution level resulting in distinguishable single colonies were counted and averaged and the number of colonies was calculated back to CFU in the original homogenate.

MelJuSo cell culture conditions

MelJuSo cell line was maintained at 37 °C/5% CO2 in Gibco Iscove's Modified Dulbecco's Medium (IMDM, Life Technologies-Invitrogen) supplemented with 10% fetal bovine serum (FBS, Greiner Bio-One, Alphen a/d Rijn, The Netherlands), 100 units/ml Penicillin and 100 µg/ml Streptomycin (Life Technologies-Invitrogen).

Infection of MelJuSo cells

MelJuSo cells were seeded in 96-well flat-bottom plates at a density of 10.000 cells/well one day prior to infection and subsequently inoculated with 100 µl of bacterial suspension at multiplicity of infection (MOI) 20, centrifuged for 3 minutes at 800 rpm and incubated at 37 °C/5% CO2 for 60 minutes. Accuracy of bacterial density measurements was verified by a standard colony-forming unit (CFU) assay. Plates were subsequently washed with culture medium containing 30 µg/ml gentamicin sulfate (Lonza BioWhittaker, Basel, Switzerland), incubated for 10 minutes, washed, and incubated at 37 °C/5% CO2 in medium containing 5 µg/ml gentamicin and indicated compounds until readout.

Compound treatment of infected MelJuSo cells
Infected cells were treated overnight with chemical compounds at a 10 µM concentration in medium containing 5 µg/ml gentamicin.

Flow cytometry
Mm infected MelJuSo cells were washed with PBS after 24 hours of compound treatment, harvested using 50 µl of Trypsin-EDTA 0.05% (ThermoFisher Scientific, Waltham, MA, USA) and added to 100 µl of 1% para-formaldehyde (PFA) (Pharmacy LUMC, the Netherlands). Cells were fixed for 1 hour prior to acquisition on a FACSCalibur using a High Throughput Sampler (HTS) (BD BioSciences).

Statistical analysis and data transformation
Due to experimental variation caused by biological variation, data of multiple experiments was combined. When data was combined, it was normalized to the mean of the control group of that experiment and normalized data of multiple experiments was combined. The number of experiments combined is described for each experiment. In the case of *Stm,* CFU count data was log-transformed. For all analysis a non-parametric distribution was assumed. The statistical test performed for each experiment is described in the figure legend. All statistical tests were performed using GraphPad Prism version 7.0.

Acknowledgements

This project was funded by NWO Domain Applied and Engineering Sciences (NWO-TTW grant 13259). The funders had no role in study design, data collection and analysis, decision to publish, or preparation of the manuscript. The authors declare that they have no conflicting interests.

References

1. An, W. F. & Tolliday, N. Cell-based assays for high-throughput screening. *Mol. Biotechnol.* **45**, 180–186 (2010).

2. Kumar, D. *et al.* Genome-wide analysis of the host intracellular network that regulates survival of Mycobacterium tuberculosis. *Cell* **140**, 731–43 (2010).

3. Korbee, C. J. *et al.* Combined chemical genetics and data-driven bioinformatics approach identifies receptor tyrosine kinase inhibitors as host-directed antimicrobials. *Nat. Commun.* **9**, 358 (2018).

4. Wang, L. *et al.* High-Throughput Functional Genetic and Compound Screens Identify Targets for Senescence Induction in Cancer. *Cell Rep.* **21**, 773–783 (2017).

5. Wilkinson, G. F. & Pritchard, K. In vitro screening for drug repositioning. *J. Biomol. Screen.* **20**, 167–179 (2015).

6. Madrid, P. B. *et al.* A Systematic Screen of FDA-Approved Drugs for Inhibitors of Biological Threat Agents. *PLoS One* **8**, e60579 (2013).

7. Younis, W., Thangamani, S. & Seleem, M. N. Repurposing Non-Antimicrobial Drugs and Clinical Molecules to Treat Bacterial Infections. *Curr. Pharm. Des.* **21**, 4106–11 (2015).

8. Barrows, N. J. *et al.* A Screen of FDA-Approved Drugs for Inhibitors of Zika Virus Infection. *Cell Host Microbe* **20**, 259–270 (2016).

9. Amoedo, N. D., Obre, E. & Rossignol, R. Drug discovery strategies in the field of tumor energy metabolism: Limitations by metabolic flexibility and metabolic resistance to chemotherapy. *Biochim. Biophys. Acta - Bioenerg.* **1858**, 674–685 (2017).

10. Costa, A., Sarmento, B. & Seabra, V. An evaluation of the latest in vitro tools for drug metabolism studies . *Expert Opin. Drug Metab. Toxicol.* **10**, 103–119 (2013).

11. Patton, E. E. & Tobin, D. M. Spotlight on zebrafish: the next wave of translational research. *Dis. Model. Mech.* **12**, dmm039370 (2019).

12. Lieschke, G. J. & Currie, P. D. Animal models of human disease: Zebrafish swim into view. *Nat. Rev. Genet.* **8**, 353–367 (2007).

13. Cornet, C., Di Donato, V. & Terriente, J. Combining Zebrafish and CRISPR/Cas9: Toward a more efficient drug discovery pipeline. *Front. Pharmacol.* **9**, 1–11 (2018).

14. Stainier, D. Y. R. *et al.* Guidelines for morpholino use in zebrafish. *PLoS Genet.* **13**, 6–10 (2017).

15. Page, D. M. *et al.* An evolutionarily conserved program of B-cell development and activation in zebrafish. *Blood* **122**, 1–12 (2013).

16. Meijer, A. & Spaink, H. Host-pathogen interactions made transparent with the zebrafish model. *Curr. Drug Targets* 1000–1017 (2011).

17. Cui, C. *et al. Infectious disease modeling and innate immune function in zebrafish embryos. Methods in cell biology* vol. 105 (Elsevier Inc., 2011).

18. Tobin, D. M., May, R. C. & Wheeler, R. T. Zebrafish: A See-Through Host and a Fluorescent Toolbox to Probe Host–Pathogen Interaction. *PLoS Pathog.* **8**, e1002349 (2012).

19. Torraca, V., Masud, S., Spaink, H. P. & Meijer, A. H. Macrophage-pathogen interactions in infectious diseases: new therapeutic insights from the zebrafish host model. *Dis. Model. Mech.* **7**, 785–97 (2014).

20. Yoshida, N., Frickel, E. M. & Mostowy, S. Macrophage-microbe interactions: Lessons from the Zebrafish model. *Front. Immunol.* **8**, (2017).

21. Hawn, T. R., Matheson, A. I., Maley, S. N. & Vandal, O. Host-directed therapeutics for tuberculosis: can we harness the host? *Microbiol. Mol. Biol. Rev.* **77**, 608–27 (2013).

22. Guler, R. & Brombacher, F. Host-directed drug therapy for tuberculosis. *Nat. Chem. Biol.* **11**, 748–751 (2015).

23. Hawn, T. R., Shah, J. A. & Kalman, D. New tricks for old dogs: Countering antibiotic resistance in tuberculosis with host-directed therapeutics. *Immunol. Rev.* **264**, 344–362 (2015).

24. Zumla, A., Rao, M., Dodoo, E. & Maeurer, M. Potential of immunomodulatory agents as adjunct host-directed therapies for multidrug-resistant tuberculosis. *BMC Med.* **14**, 1–12 (2016).

25. Davis, J. M. *et al.* Real-time visualization of Mycobacterium-macrophage interactions leading to initiation of granuloma formation in zebrafish embryos. *Immunity* **17**, 693–702 (2002).

26. Ramakrishnan, L. The Zebrafish Guide to Tuberculosis Immunity and Treatment. *Cold Spring Harb. Symp. Quant. Biol.* **78**, 179–192 (2013).

27. Meijer, A. H. Protection and pathology in TB: learning from the zebrafish model. *Semin. Immunopathol.* **38**, 261–273 (2016).

28. Ramakrishnan, L. Revisiting the role of the granuloma in tuberculosis. *Nat. Rev. Immunol.* **12**, 352–366 (2012).

29. Hmama, Z., Peña-Díaz, S., Joseph, S. & Av-Gay, Y. Immunoevasion and immunosuppression of the macrophage by Mycobacterium tuberculosis. *Immunol. Rev.* **264**, 220–232 (2015).

30. McClean, C. M. & Tobin, D. M. Macrophage form, function, and phenotype in mycobacterial infection: Lessons from tuberculosis and other diseases. *Pathog. Dis.* **74**, 1–15 (2016).

31. Cadena, A. M., Fortune, S. M. & Flynn, J. L. Heterogeneity in tuberculosis. *Nat. Rev. Immunol.* **17**, 691–702 (2017).

32. Veneman, W. & Stockhammer, O. A zebrafish high throughput screening system used for Staphylococcus epidermidis infection marker discovery. *BMC …* 1–15 (2013).

33. Carvalho, R. *et al.* A high-throughput screen for tuberculosis progression. *PLoS One* **6**, e16779 (2011).

34. Kuijl, C., Savage, N., Marsman, M. & Tuin, A. Intracellular bacterial growth is controlled by a kinase network around PKB/AKT1 (supplementary figures). *Nature* 1–27 (2007) doi:10.1038/nature0.

35. Stoop, E. J. M. *et al.* Zebrafish embryo screen for mycobacterial genes involved in the initiation of granuloma formation reveals a newly identified ESX-1 component. *Dis. Model. Mech.* **4**, 526–536 (2011).

36. Benard, E. L., Rougeot, J., Racz, P. I., Spaink, H. P. & Meijer, A. H. *Transcriptomic Approaches in the Zebrafish Model for Tuberculosis—Insights Into Host- and Pathogen-specific Determinants of the Innate Immune Response*. *Advances in Genetics* vol. 95 (Elsevier Ltd, 2016).

37. van der Sar, A. M. *et al.* Zebrafish embryos as a model host for the real time analysis of Salmonella typhimurium infections. *Cell. Microbiol.* **5**, 601–611 (2003).

38. Benard, E. L. *et al.* Infection of zebrafish embryos with intracellular bacterial pathogens. *J. Vis. Exp.* 1–8 (2012) doi:10.3791/3781.

39. Masud, S. *et al*. Macrophages target Salmonella by Lc3-associated phagocytosis in a systemic infection model. *Autophagy* **00**, 1–17 (2019).

40. Takaki, K., Davis, J. M., Winglee, K. & Ramakrishnan, L. Evaluation of the pathogenesis and treatment of Mycobacterium marinum infection in zebrafish. *Nat. Protoc.* **8**, 1114–24 (2013).

41. Yang, R. *et al*. Miconazole protects blood vessels from MMP9-dependent rupture and hemorrhage. *Dis. Model. Mech.* **10**, 337–348 (2017).

42. Tseng, W.-C. *et al*. Modeling Niemann-Pick disease type C1 in zebrafish: a robust platform for in vivo screening of candidate therapeutic compounds. *Dis. Model. Mech.* **11**, dmm034165 (2018).

43. Delgadillo-Silva, L. F. *et al*. Modelling pancreatic β-cell inflammation in zebrafish identifies the natural product wedelolactone for human islet protection. *Dis. Model. Mech.* **12**, dmm036004 (2019).

44. Matty, M. A. *et al*. Potentiation of P2RX7 as a host-directed strategy for control of mycobacterial infection. *Elife* **8**, 1–27 (2019).

45. Traver, D. *et al*. The zebrafish as a model organism to study development of the immune system. *Adv. Immunol.* **81**, 253–330 (2003).

46. van der Sar, A. M. *et al*. Mycobacterium marinum Strains Can Be Divided into Two Distinct Types Based on Genetic Diversity and Virulence. *Infect. Immun.* **72**, 6306–6312 (2004).

47. Butts, A. *et al*. Estrogen receptor antagonists are anti-cryptococcal agents that directly bind EF hand proteins and synergize with fluconazole in vivo. *MBio* **5**, 1–11 (2014).

48. Dittmar, A. J., Drozda, A. A. & Blader, I. J. Drug Repurposing Screening Identifies Novel Compounds That Effectively Inhibit Toxoplasma gondii growth. *mSphere* **1**, 1–15 (2016).

49. Miguel, D. C., Yokoyama-Yasunaka, J. K. U. & Uliana, S. R. B. Tamoxifen is effective in the treatment of Leishmania amazonensis infections in mice. *PLoS Negl. Trop. Dis.* **2**, (2008).

50. Chen, F. C. *et al*. Pros and cons of the tuberculosis drugome approach - An empirical analysis. *PLoS One* **9**, (2014).

51. Jang, W. S. *et al*. Anti-mycobacterial activity of tamoxifen against drug-resistant and intra-macrophage Mycobacterium tuberculosis. *J. Microbiol. Biotechnol.* **25**, 946–950 (2015).

52. Pattingre, S., Bauvy, C., Levade, T., Levine, B. & Codogno, P. Ceramide-induced autophagy: To junk or to protect cells? *Autophagy* **5**, 558–560 (2009).

53. Gutierrez, M. G. *et al*. Autophagy is a defense mechanism inhibiting BCG and Mycobacterium tuberculosis survival in infected macrophages. *Cell* **119**, 753–766 (2004).

54. Yang, Z. & Klionsky, D. J. Mammalian autophagy: Core molecular machinery and signaling regulation. *Curr. Opin. Cell Biol.* **22**, 124–131 (2010).

55. Deretic, V., Saitoh, T. & Akira, S. Autophagy in infection, inflammation and immunity. *Nat. Rev. Immunol.* **13**, 722–37 (2013).

56. MacMicking, J. D. *et al*. Identification of nitric oxide synthase as a protective locus against tuberculosis. *Proc. Natl. Acad. Sci.* **94**, 5243–5248 (1997).

57. Elks, P. M., Renshaw, S. a., Meijer, a. H., Walmsley, S. R. & van Eeden, F. J. Exploring the HIFs, buts and maybes of hypoxia signalling in disease: lessons from zebrafish models. *Dis. Model. Mech.* **8**, 1349–1360 (2015).

58. Jamaati, H. *et al.* Nitric oxide in the pathogenesis and treatment of tuberculosis. *Front. Microbiol.* **8**, 1–11 (2017).

59. Lin, C. W. *et al.* Amiodarone as an autophagy promoter reduces liver injury and enhances liver regeneration and survival in mice after partial hepatectomy. *Sci. Rep.* **5**, 1–13 (2015).

60. Jacquin, E. *et al.* Pharmacological modulators of autophagy activate a parallel noncanonical pathway driving unconventional LC3 lipidation. *Autophagy* **13**, 854–867 (2017).

61. Komander, D., Clague, M. J. & Urbé, S. Breaking the chains: Structure and function of the deubiquitinases. *Nat. Rev. Mol. Cell Biol.* **10**, 550–563 (2009).

62. Harrigan, J. A., Jacq, X., Martin, N. M. & Jackson, S. P. Deubiquitylating enzymes and drug discovery: Emerging opportunities. *Nat. Rev. Drug Discov.* **17**, 57–77 (2018).

63. Zhang, R. *et al.* The selective autophagy receptors Optineurin and p62 are both required for zebrafish host resistance to mycobacterial infection. *PLOS Pathog.* **15**, e1007329 (2019).

64. Mesquita, F. S. *et al.* The Salmonella deubiquitinase SseI inhibits selective autophagy of cytosolic aggregates. *PLoS Pathog.* **8**, (2012).

65. Ramakrishnan, L., Federspiel, N. A. & Falkow, S. Granuloma-Specific Expression of Mycobacterium Virulence Proteins from the Glycine-Rich PE-PGRS Family Lalita Ramakrishnan, Nancy A. Federspiel, and Stanley Falkow Supplementary Material DFI Methods: **288**, 300 (2000).

66. Chan, K. *et al.* Complex pattern of Mycobacterium marinum gene expression during long-term granulomatous infection . *Proc. Natl. Acad. Sci.* **99**, 3920–3925 (2002).

67. Sundaramurthy, V. *et al.* Integration of chemical and RNAi multiparametric profiles identifies triggers of intracellular mycobacterial killing. *Cell Host Microbe* **13**, 129–42 (2013).

68. Napier, R. J. *et al.* Imatinib-Sensitive tyrosine kinases regulate mycobacterial pathogenesis and represent therapeutic targets against tuberculosis. *Cell Host Microbe* **10**, 475–485 (2011).

69. Challa, A. K. & Chatti, K. Conservation and Early Expression of Zebrafish Tyrosine Kinases Support the Utility of Zebrafish as a Model for Tyrosine Kinase Biology. *Zebrafish* **10**, 264–274 (2012).

70. de Koning, C. *et al.* Visualizing Compound Distribution during Zebrafish Embryo Development: The Effects of Lipophilicity and DMSO. *Birth Defects Res. Part B - Dev. Reprod. Toxicol.* **104**, 253–272 (2015).

71. Kantae, V. *et al.* Pharmacokinetic Modeling of Paracetamol Uptake and Clearance in Zebrafish Larvae: Expanding the Allometric Scale in Vertebrates with Five Orders of Magnitude. *Zebrafish* **13**, 504–510 (2016).

72. van Wijk, R. C. *et al.* Impact of post-hatching maturation on the pharmacokinetics of paracetamol in zebrafish larvae. *Sci. Rep.* **9**, 2149 (2019).

73. Hoiseth, S. K. & Stocker, B. A. Aromatic-dependent Salmonella typhimurium are non-virulent and effective as live vaccines. *Nature* **291**, 238–239 (1981).

74. Burton, N. A. *et al.* Disparate impact of oxidative host defenses determines the fate of salmonella during systemic infection in mice. *Cell Host Microbe* **15**, 72–83 (2014).